SMB Enantioseparation: Process Development, Modeling, and Operating Conditions

Sylvie Lehoucq and Didier Verhève
Chaire de Technologie Chimique (FWSE), Université de Mons-Hainaut, 7000 Mons, Belgium

Alain Vande Wouwer
Laboratoire d'Automatique, Faculté Polytechnique de Mons, 7000 Mons, Belgium

Emile Cavoy
Drug Discovery, UCB Pharma Sector s.a., B1420 Braine-l'Alleud, Belgium

The design of a simulated moving bed (SMB) pilot used for chiral drug separation is presented. On-line concentration measurements allow the observation of detailed concentration profiles along the SMB columns. Based on an extensive set of experimental data, an equivalent countercurrent model was derived. In this model, mass-transfer kinetics are described by linear driving-force models, while the equilibrium concentrations are given by modified competitive Langmuir isotherms. The isotherm parameters are estimated using a peak fitting procedure, which starts with initial values given by a simple retention-time method. The dispersion phenomena are estimated through the variation of the HETP with the fluid-phase velocity. The good agreement between the model and the real system is demonstrated by several cross-validation results corresponding to the separation of given racemic mixtures under various operating conditions. The model defines a zone of complete separation and allows optimal operating conditions to be selected.

Introduction

The trend of the pharmaceutical sector toward commercializing chiral drugs as pure enantiomers enhances the need of efficient processes for the separation of racemates. Chiral chromatography has been extensively used for chiral separations in the analytical field. Chiral phases are, however, very expensive and their use for preparative or industrial purposes has long been avoided. In the beginning of the 1990s (Negawa and Shoji, 1992), it was shown that significant benefits in terms of chiral phase and solvent consumption could be achieved by performing the separation with a simulated moving-bed (SMB) process. In such a system, a countercurrent movement of the liquid and solid phases is simulated in order to increase the exchange capabilities between the two phases.

Figure 1 shows the equivalent countercurrent representation of a typical SMB. The system consists of four zones, each with constant flow rate, that are delimited by the several material flow inlets and outlets. The feed to separate is introduced between zones 2 and 3. The component with less affinity for the solid phase (the raffinate) is collected between zones 3 and 4, and the most retained component (the extract) is collected between zones 1 and 2. Fresh solvent is introduced between zones 4 and 1 to regenerate the solid phase. Part of the liquid phase is recycled to zone 1 after being washed in zone 4. To avoid problems associated with the movement of a solid phase, each zone is subdivided into several interlinked columns and a simulated solid movement is achieved by switching, at given time intervals, the positions of the flow inlets and outlets in the direction of the liquid-phase flow.

In the following, the major features of an in-house developed SMB pilot (Cavoy et al., 1997) are described. This pilot is dedicated to the separation of racemates prior to clinical tests. It can also be used for a first evaluation of the feasibility of an up-scaled separation. The given design is flexible, features some useful monitoring devices, and achieves very efficient separations.

Correspondence concerning this article should be addressed to A. Vande Wouwer.

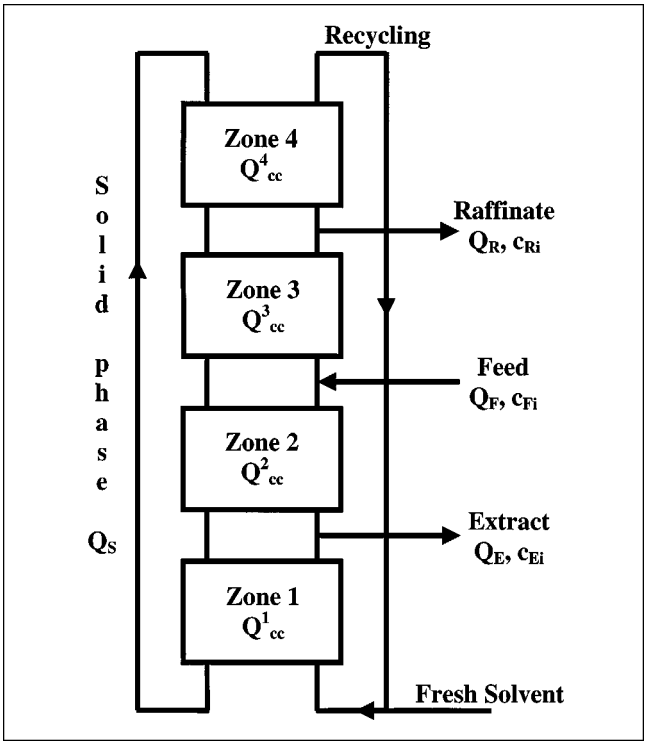

Figure 1. Equivalent countercurrent representation of a SMB.

To operate this SMB pilot, five input variables, that is, four liquid-phase flow rates and the switching period, must be selected so as to achieve the desired purity of the separated enantiomers in an optimal way. This problem is highly related to the equilibrium governing the separation. With low-capacitive chiral phases, the equilibrium is described by nonlinear competitive isotherms whose determination will be of primary importance.

The experimental results reported in this study correspond to the separation of two different racemic mixtures (denoted 1 and 2, respectively, in the continuation of the text) under various operating conditions. For confidentiality reasons, the exact nature of these components cannot be divulged. It can only be said that they differ significantly by their molecular weight and chemical structure and that they are characterized by different nonlinear equilibrium isotherms.

In the first part of this study, a simulation program based on an equivalent countercurrent model is developed. This model is described by a set of convection–dispersion partial differential equations (PDEs) that contain several unknown parameters: column porosity, dispersion coefficients, mass-transfer coefficients, and isotherm parameters. A step-by-step procedure for the experimental determination of these parameters is given. In particular, the isotherm parameters are estimated using a peak fitting procedure, which starts with initial values given by a simple retention time method (RTM).

Based on an extensive set of experimental data, the good agreement between the model and the real system is demonstrated both in direct and cross-validation.

In the second part of this study, a procedure for selecting optimal operating conditions is discussed. Based on the determination of a zone of complete separation (Mazzotti et al., 1997), the product purity predicted for different operating conditions is compared with experimental results. In addition, the simulation program is used to investigate other important issues, including the influence of the feed concentration on the zone of complete separation and the selection of the number of columns in each zone according to dispersion effects.

In contrast with a recent study (Francotte et al., 1998), experimental results demonstrate that the raffinate productivity can be significantly increased by operating the SMB process outside the zone of complete separation, in a region where only pure raffinate can be obtained.

Finally, the last section of this article is devoted to some conclusions.

System Design

Because the separation process is very sensitive to flow-rate variations, the system has been designed so as to guarantee an accurate regulation of the material flow rates. In this regard, the SMB unit, which is illustrated in Figure 2, features several novel technical characteristics:

- The extract and raffinate are withdrawn by two values. A PID control scheme allows the outlet flow rates, which are measured by two Coriolis mass flowmeters, to be regulated by acting on the valve apertures. Actually, because the system is under pressure, a valve regulation is easier to implement than a pump regulation involving the introduction of some counterpressure at the outlet of the pump.
- The bottom of each column is connected either to the recycling line or to the top of the next column via a three-port valve. This additional valve allows the recycling pump to be placed out of the SMB zones. This design is particularly advantageous, since the pump runs at a constant flow rate. On the other hand, when the recycling pump is placed between two of the columns in the line connecting them, its flow rate must change depending on the zone where the columns are located.

For satisfactory process operation, the several columns must be as identical as possible. In the SMB pilot considered in this study, columns are fitted out with a piston allowing a good packing reproducibility. Figure 3 shows the comparison of the chromatograms measured after injection of a test product in each of the twelve columns of the SMB unit (Merk 4.8 cm ID and 11.6 cm in length, packed with a chiral phase from Daicel Chemical Industries, Ltd.). In this figure, the first peak corresponds to a component that is not retained by the chiral adsorbent (in this case 1,3,5-tri-*tert*-butylbenzene), whereas the two following peaks correspond to the components of a racemic mixture. These chromatograms are nearly identical, demonstrating the excellent packing reproducibility.

In addition to these technical features, some monitoring devices have been implemented:

- A UV detector is connected to the inlet of the recycling pump. Under normal separation conditions, the liquid flowing through the recycling pump must be pure solvent and the UV signal must be flat. Any change in the UV signal is thus an indicator of a problem either due to system perturbations (flow-rate perturbation, temperature change, and so on) or

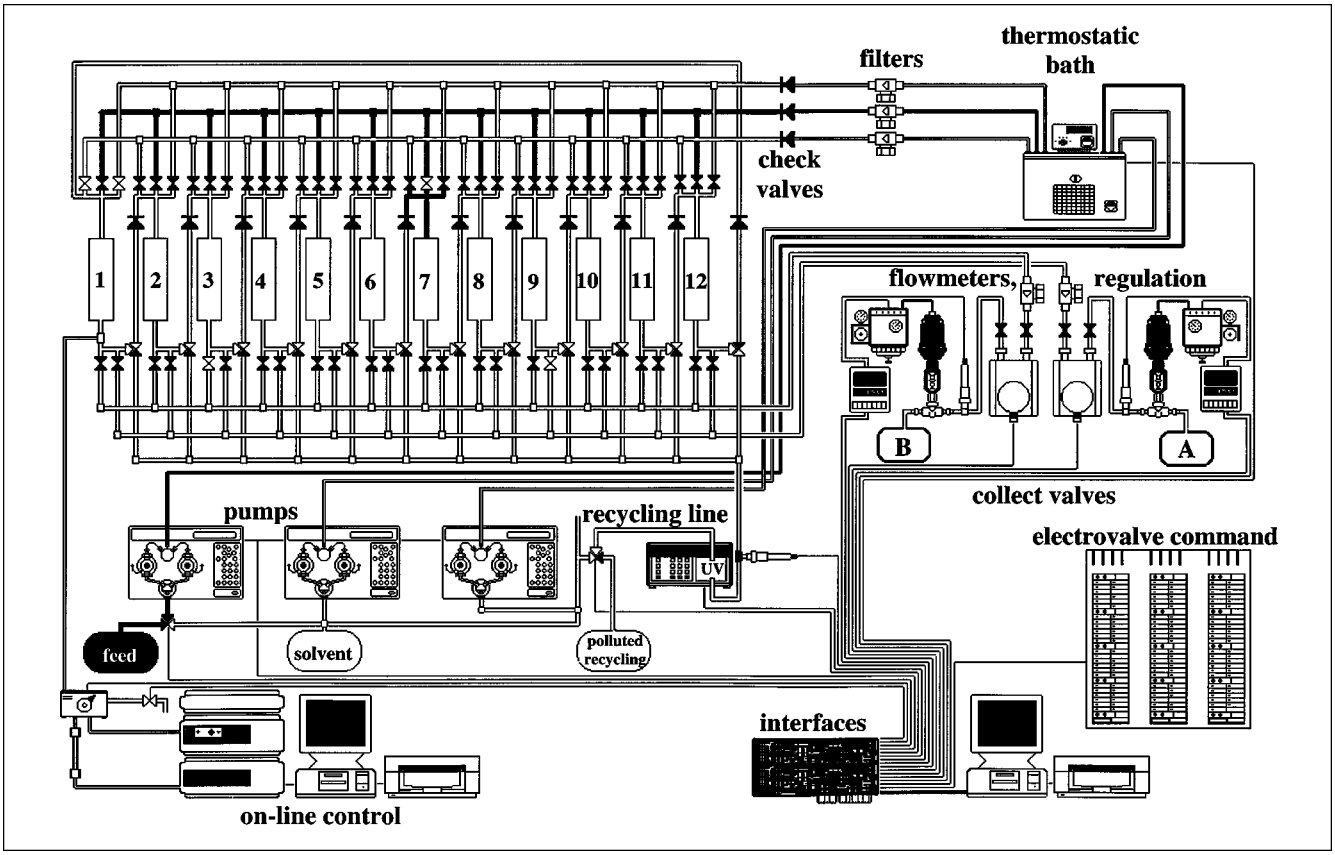

Figure 2. SMB pilot.

fault (column degradation, and so on) or due to a wrong choice in the operating conditions. During the time needed to check and resolve the problem, the recycling flow can be deviated to a waste, and instead some fresh solvent can be injected in zone 1. This precaution avoids propagating the pollution into all the system, and hence allows a quicker resolution of the problem.

- A monitoring of the separation process is performed on-line. A small part of the liquid flowing out of column 1 is deviated to a capillary tube connected to an on/off valve through a Rheodyne valve (Figure 4). At a given percentage of the switching period Δt, the on/off valve is open and the capillary tube as well as the injection loop connected to the Rheodyne valve are filled with the flow exiting column 1 (Rheodyne valve in load position, Figure 4a). When the loop is full, the on/off valve is closed and the Rheodyne valve is put in the injection position (Figure 4b); the content of the loop is injected to an analytical column, and the components are separated. This way, the composition of the flow exiting

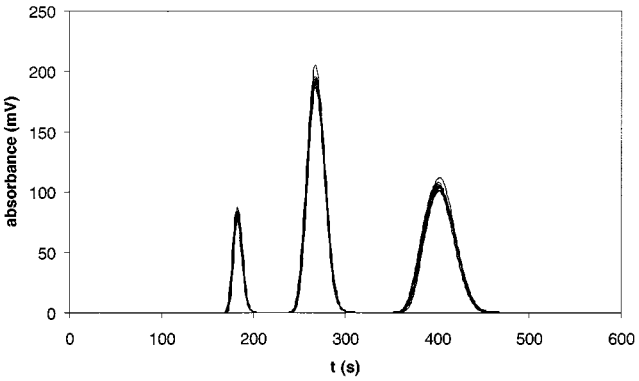

Figure 3. Packing reproducibility.

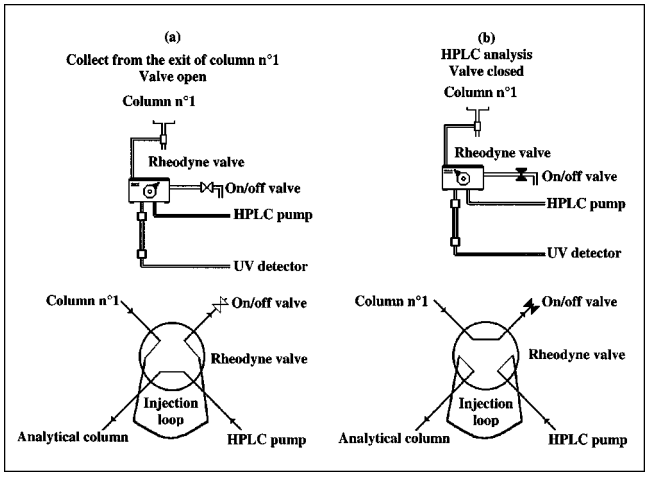

Figure 4. Valve setting for on-line analysis.

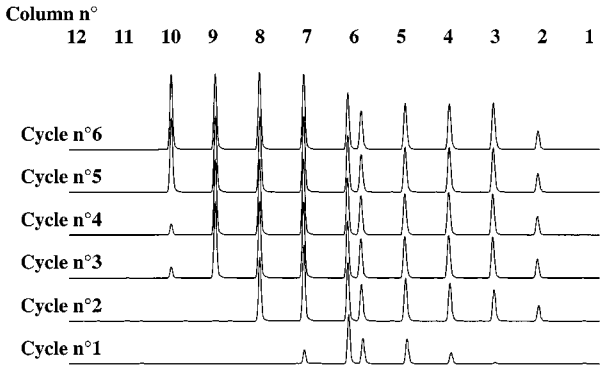

Figure 5. On-line analysis at 50% of the switching period Δt.

First 6 cycles of the SMB separation of racemic mixture 1 with $c_F = 40$ g/L. 2-4-4-2 SMB configuration, $\Delta t = 100$ s, $Q^1 = 202$ mL/min, $Q_E = 75$ mL/min, $Q_R = 24$ mL/min, $Q_F = 18.5$ mL/min.

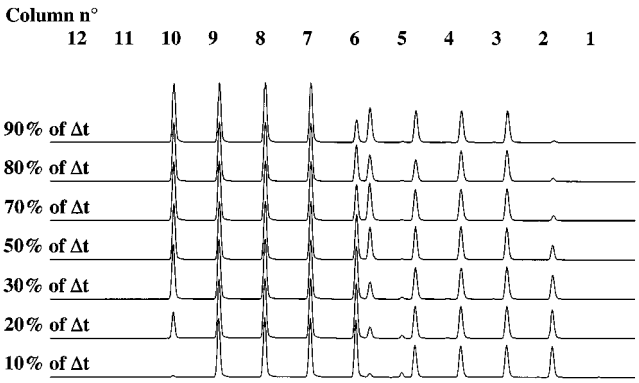

Figure 6. On-line analysis at different percentages of the switching period Δt.

Steady-state separation of racemic mixture 1 with $c_F = 40$ g/L. Same conditions as in Figure 5.

column 1 at a given percentage of the switching period is determined on-line. During a cycle, column 1 successively occupies twelve different positions so that it is possible to observe the evolution of the separation along the SMB system. The sample needed for the on-line analysis is only 1.2 μL—a negligible quantity compared to the SMB holdup—so that the concentration profiles are unaffected.

For example, Figure 5 shows the twelve chromatograms measured at 50% of the switching period, during each of the first six cycles of a separation of racemic mixture 1. For each cycle, the first measurement (to the left in Figure 5) is performed when column 1 is in position 12.

Thanks to these on-line analyses, it is possible to detect when steady-state conditions are reached. In the example under consideration, the chromatograms measured during the fifth and sixth cycles are almost identical, which means that the SMB pilot operates in steady state after 5 to 6 cycles.

Under these conditions, it is possible to observe more detailed separation profiles by performing the analyses at different percentages of the switching period. Figure 6 shows seven consecutive cycles and the twelve chromatograms measured at 10%, 20%, 30%, 50%, 70%, 80%, and 90% of the switching period, respectively.

The area of the peaks can be used to draw internal concentration profiles, as illustrated in Figure 7, which compares, for a separation of racemic mixture 2, detailed concentration profiles with those obtained from analyses at 50% of the switching period only. The detailed profiles clearly show a concentration front for the raffinate (component A) and a concentration plate for the extract (component B). These characteristics could not be observed from the profile at 50%.

These monitoring devices will be useful to check the validity of the mathematical models developed in the next section.

System Modeling

There are several approaches for modeling an SMB process (Ruthven and Ching, 1989). The one selected in this study assumes an equivalent countercurrent movement of the solid phase. This so-called true moving-bed (TMB) model neglects the dynamics associated with periodic switching and produces mean concentration profiles over a switching period. Theoretically, the TMB model describes the situation existing in an SMB process with infinitely many columns in each zone. However, experience shows that this simplifying assumption holds true in the case of relatively coarse subdivisions, for example, 2–4 columns in each zone (Pais et al., 1998).

As we will see in the following, this simple approach is sufficient for the purposes of the present study, that is, the experimental development of a simulation model (including parameter estimation and model validation) and the selection of operating conditions. A more rigorous approach, involving a representation of the system as an arrangement of static chromatographic columns and taking into account periodic switching, would be required to investigate system dynamics in more depth and to design control schemes. These issues are currently being addressed by the authors and will be reported elsewhere.

Following the TMB approach, a model is developed based on the additional assumption that the system is one-dimensional, that is, velocities and concentrations are radially homogeneous, so that the mass balances for each component of a racemic mixture can be expressed by convection–dispersion PDEs in the form

$$\frac{\partial c_i}{\partial t} + \frac{1-\epsilon}{\epsilon}\frac{\partial q_i}{\partial t} = D_{Li}\frac{\partial^2 c_i}{\partial z^2} - u_{cc}^j\frac{\partial c_i}{\partial z} + \frac{1-\epsilon}{\epsilon}u_s\frac{\partial q_i}{\partial z}$$
$$i = A,\ B,\ j = 1,\ \ldots,\ 4, \quad (1)$$

where c_i is the concentration of the component i in the liquid phase, and q_i is the corresponding concentration in the solid phase. The parameter ϵ is the bed porosity (total void fraction), D_{Li} represents the axial dispersion coefficient, and u_{cc}^j and u_s denote the liquid phase velocity in zone j and the solid phase velocity, respectively. These countercurrent velocities are related to the SMB operating parameters by

$$u_s = \frac{L}{\Delta t}, \qquad u_{cc}^j = \frac{Q_{cc}^j}{\epsilon\Sigma} = \frac{Q^j}{\epsilon\Sigma} - \frac{L}{\Delta t} \qquad j = 1,\ \ldots,\ 4, \quad (2)$$

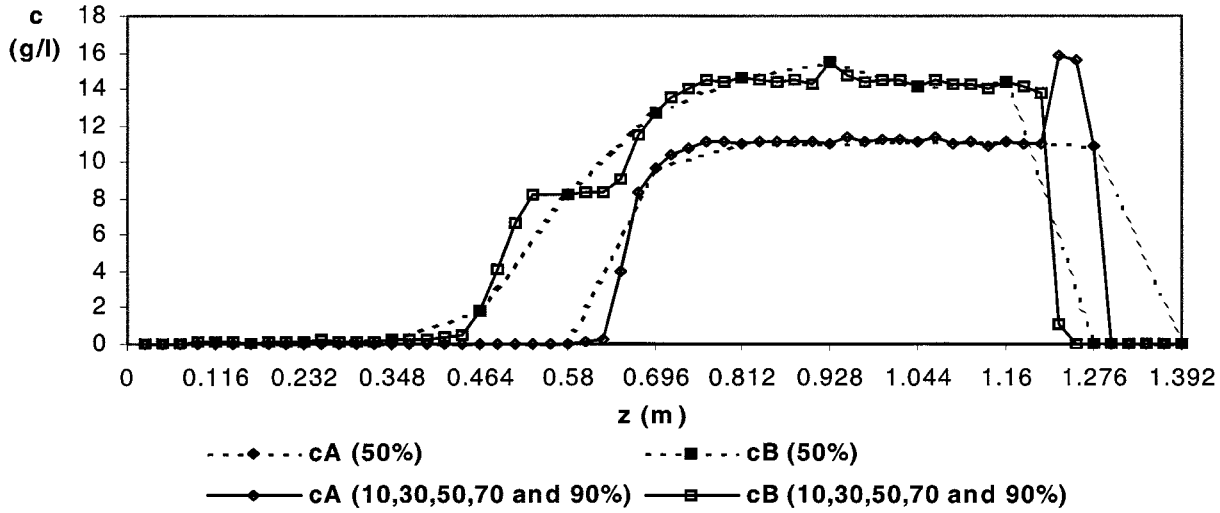

Figure 7. Significance of detailed experimental profiles.

SMB separation of racemic mixture 2. Configuration 4-2-5-1; $\Delta t = 75$ s; $Q^1 = 294$ mL/min; $Q_E = 137.5$ mL/min; $Q_R = 47.3$ mL/min; $Q_F = 22$ mL/min.

where L is the length of a single chromatographic column, Δt is the switching period, Q_{cc}^j is the countercurrent liquid flow rate in zone j, Q^j is the SMB liquid flow rate in zone j, and Σ is the cross-section area of a chromatographic column.

Further, a lumped kinetic model expresses the accumulation rate of the components in the solid phase due to a mass-transfer driving force. Here, a linear driving-force (LDF) model (Ruthven, 1984) is selected,

$$\frac{\partial q_i}{\partial t} = u_s \frac{\partial q_i}{\partial z} + k_{FSi}(q_i^* - q_i) \qquad i = A, B, \tag{3}$$

where k_{FSi} is the overall mass-transfer coefficient existing in a film around the sorbent particles and q_i^* is the solid-film equilibrium concentration, which is related to the liquid-phase concentrations (c_A, c_B) by an adsorption equilibrium relation.

Adsorption on chiral phases is known to be well described by modified Langmuir isotherms (Nicoud and Seidel-Morgenstern, 1996), that is,

$$q_i^* = \lambda c_i + \frac{q_s b_i c_i}{1 + b_A c_A + b_B c_B} \qquad i = A, B, \tag{4}$$

where λ, q_s, b_A, and b_B are the modified Langmuir isotherm parameters.

Equations 1 to 4, supplemented with initial and boundary conditions, are solved numerically using the method of lines (Schiesser, 1991). First, the spatial derivatives are approximated using finite difference schemes on nonuniform spatial grids, that is, more grid points are concentrated near the several zone boundaries where steep concentration gradients take place. Then, the resulting set of semidiscrete ODEs is integrated in time using the backward differentiation formula (BDF) solver LSODES (Hindmarsh, 1983), which can automatically generate the sparsity pattern of the Jacobian matrix. This feature is particularly interesting in this application in which the Jacobian matrix has a special structure involving elements located off the band around the main diagonal, near the matrix corners (arising from material recycling in the SMB process).

Parameter Estimation

The model equations contain several unknown parameters, for example, bed porosity, isotherm parameters, dispersion coefficients, and mass-transfer coefficients, whose numerical values must be inferred from experimental data.

Bed porosity

A component, which is not retained by the chiral phase (1,3,5-tri-*tert*-butylbenzene was used in this study), is injected in one of the SMB columns. The bed porosity or total void fraction can easily be computed from the measured retention time t_0 (see Figure 3, in which t_0 corresponds to the retention time of the first peak)

$$\epsilon = \frac{Q_v t_0}{V} \tag{5}$$

where Q_v is the liquid flow rate and V is the column volume.

Isotherm parameters

Isotherm parameters are determined by a combined procedure in which a simple retention-time method (RTM) (Guiochon et al., 1994) provides initial parameter estimates for a peak-fitting algorithm.

Experiments are performed using N_c (typically 2) columns of the SMB connected in series and used in batch mode. Different quantities of racemic mixture are injected and the chromatograms are recorded.

First, small quantities of racemic mixtures are injected so that the equilibrium relation corresponds to the linear part of the Langmuir isotherms characterized by slopes equal to $\lambda +$

$q_s b_A$ and $\lambda + q_s b_B$, respectively. These values can be obtained from the retention times, $t_{R_0,A}$ and $t_{R_0,B}$, of the peaks (Guiochon et al., 1994)

$$k'_{0,i} = \frac{t_{R_0,i} - t_0}{t_0} = \frac{1-\epsilon}{\epsilon}(\lambda + q_s b_i), \qquad i = A, B, \quad (6)$$

where $t_0 = (N_c L)/u$ is the transportation lag of the columns and u is the liquid-phase velocity.

Then, larger quantities of racemic mixtures are injected, resulting in very sharp peaks (near shocks) traveling through the chromatographic columns. The terms $q_s b_i$ can be computed, at least approximately, from the retention times of the shocks (Guiochon et al., 1994)

$$t_{R_{\text{shock}},i} = t_p + t_{R_0,i} + \frac{1-\epsilon}{\epsilon} q_s b_i t_0 \left(L_{f,i} - 2\sqrt{L_{f,i}} \right),$$
$$L_{f,i} = \frac{n_i}{(1-\epsilon) V q_s} \qquad i = A, B, \quad (7)$$

where n_i is the mass injected and t_p is the duration of the injection.

Based on (at least) two injections, Eqs. 6–7 allow the several unknown parameters, λ, q_s, b_A, b_B, to be determined. It is not expected that this method, which is based on the solution of the ideal model of chromatography (no dispersion and mass-transfer resistance), is very accurate, since it assumes no interaction between the two component peaks (which is not true when the equilibrium relation is nonlinear). However, it quickly gives a first approximation of the isotherm parameter values, which can then be used as initial guesses in a peak-fitting algorithm.

The peak-fitting algorithm is based on the numerical solution of an equilibrium-dispersion model

$$\frac{\partial c_i}{\partial t} + \frac{1-\epsilon}{\epsilon} \frac{\partial q_i^*}{\partial t} = D_{ai} \frac{\partial^2 c_i}{\partial z^2} - u \frac{\partial c_i}{\partial z}, \quad (8)$$

where D_{ai} is an apparent dispersion coefficient that lumps together dispersion and mass-transfer kinetics. The first set of experiments, in which small quantities of racemic mixture were injected and linear chromatographic conditions were achieved, can be used to estimate the values of the dispersion coefficients (Guiochon et al., 1994), that is

$$D_{ai} = \frac{N_c L u}{2 N_i} \quad (9)$$

$$N_i = 5.54 \left(\frac{t_{R_0,i}}{W_{1/2\,i}} \right)^2, \quad (10)$$

where N_i is the number of theoretical plates and $W_{1/2\,i}$ is the width halfway up the peaks.

An output least-square (OLS) criterion measures the deviation between the measured concentrations $y_i(t)$ and the concentrations $c_i(t;\theta)$ predicted by the model equations (Eq. 8)

$$J(\theta) = \frac{1}{t_f} \int_0^{t_f} \sum_{i=A}^{B} \left[y_i(t) - c_i(t;\theta) \right]^2 dt, \quad (11)$$

where θ is the vector of unknown isotherm parameters and t_f is the duration of the experiment. The minimization of the OLS criterion with respect to the unknown parameters θ is performed with the SQP algorithm FFSQP (Zhou and Tits, 1997). The convergence of this nonlinear optimization procedure is improved by starting from the RTM estimates, which are expected to be relatively close to the minimum of the criterion.

Dispersion parameters

The parameters D_{Li} and k_{FSi} characterize axial dispersion and mass-transfer resistance, respectively. For linear isotherms, the solution of the LDF model leads to the following expression for the height equivalent to a theoretical plate (Ruthven, 1984)

$$H_i = \frac{N_c L}{N_i} = \frac{2 D_{Li}}{u} + 2 \left(\frac{k'_{0,i}}{1 + k'_{0,i}} \right)^2 \frac{u}{k'_{0,i} k_{FSi}}. \quad (12)$$

Again, N_c columns of the SMB are connected in series and several injections of a racemic mixture are performed. In each experiment, small quantities are injected so that the adsorption equilibrium relation is linear. Each injection is carried out with a different value of the liquid-phase velocity. These values are chosen so as the include the range of velocities $u_s + u_{cc}^j$ expected when running the SMB system. In each case, the values of $k'_{0,i}$ and H_i are estimated from the chromatograms, based on Eqs. 6 and 10. $H_i u$ is then plotted against u^2 to give D_{Li} (from the intercept) and k_{FSi} (from the slope).

Case study and experimental validation

The several parameters estimated by the procedures just mentioned are given in Table 1 for racemic mixtures 1–2, respectively.

In both cases, the estimated values of the dispersion coefficients D_{LA} and D_{LB} are very small. Using these parameter values in the model equations (Eqs. 1–4), internal concentration profiles are computed that are steeper than the experimental observations. Actually, axial dispersion in the SMB columns appears negligible compared to dispersion effects resulting from the discretization of the SMB into twelve columns (dispersion in the interconnecting lines and valves, etc.). These latter effects can be taken into account by increasing D_{LA} and D_{LB} to $3 \cdot 10^{-6}$ m^2/s in the case of racemic mixture 1 ($3 \cdot 10^{-6}$ m^2/s and $4 \cdot 10^{-6}$ m^2/s, respectively, in the

Table 1. Model Parameters

Racemic Mixture 1	Racemic Mixture 2
$\epsilon = 0.66$	$\epsilon = 0.66$
$\lambda = 0.317$	$\lambda = 0.28$
$q_S = 49.6$ g/L	$q_S = 16.97$ g/L
$b_A = 0.0166$ L/g	$b_A = 0.0399$ L/g
$b_B = 0.0471$ L/g	$b_B = 0.1601$ L/g
$D_{LA} = 2 \times 10^{-8}$ m^2/s	$D_{LA} = 3 \times 10^{-8}$ m^2/s
$D_{LB} = 1 \times 10^{-8}$ m^2/s	$D_{LB} = 4 \times 10^{-8}$ m^2/s
$k_{FSA} = 3.75$ s^{-1}	$k_{FSA} = 2.52$ s^{-1}
$k_{FSB} = 3.18$ s^{-1}	$k_{FSB} = 1.86$s^{-1}

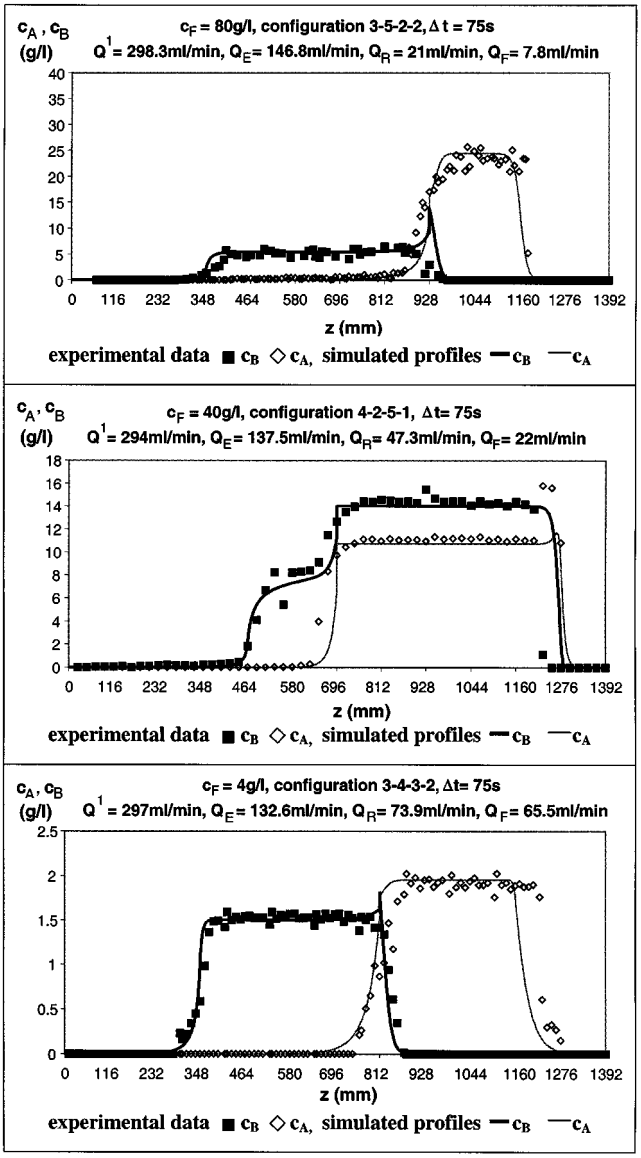

Figure 8. Experimental validation of the simulation model.

SMB separation of racemic mixture 2 under various operating conditions.

case of racemic mixture 2). This way, the discretization effects are lumped into the dispersion coefficients D_{LA} and D_{LB}.

A few experimental profiles corresponding to the separation of racemic mixture 2 under different operating conditions (flow rates, number of columns per zone, and feed concentration) are given in Figure 8 which illustrates the good agreement between the experimental and simulated profiles.

Selection of Operating Conditions

Based on the model of the SMB process derived in the previous sections, several issues related to the selection of operating conditions are now addressed.

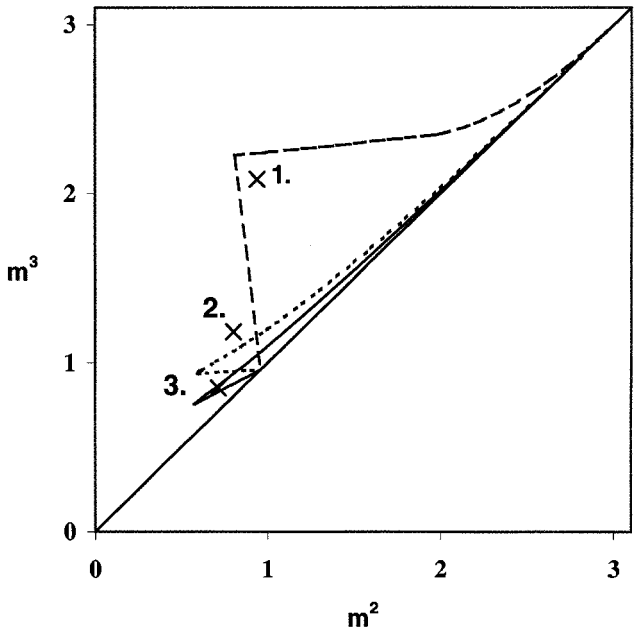

Figure 9. Zones of complete separation in the (m^2, m^3) plane for racemic mixture 2 at three different feed concentrations.

Dashed line— c_F = 4 g/L; dotted line— c_F = 40 g/L; solid line— c_F = 80 g/L.

Zone of complete separation: Selection of the several flow rates

Relative flow rates are defined as

$$m^j = \frac{Q_{cc}^j}{Q_s} \tag{13}$$

where Q_s is the countercurrent solid flow rate

$$Q_s = \frac{(1-\epsilon)\Sigma L}{\Delta t}. \tag{14}$$

In a recent study (Mazzotti et al., 1997), Mazzotti and his coworkers derived conditions on the relative flow rates leading to a complete separation of the products. These developments are based on the steady-state analytical solution of an ideal TMB model (neither dispersion nor mass-transfer resistance) in which the adsorption equilibrium is described by modified Langmuir isotherms. These conditions impose a minimum bound on m^1, which depends only on the isotherm parameters, and a maximum bound on m^4, which depends on the isotherm parameters and is a function of the relative flow rates m^2, m^3 and the feed concentration. The expressions of the conditions on m^2 and m^3 are independent of the values of m^1 and m^4 and define a triangular zone of complete separation in a plane (m^2, m^3). This zone is highly dependent on the feed concentration, as illustrated in Figure 9, which shows the complete separation zones corresponding to three different feed concentrations of racemic mixture 2.

Several operating points inside or outside the zone of complete separation are now checked experimentally. Point 1,

which corresponds to 4 g/L feed concentration, is in the complete separation zone and leads effectively to pure extract and raffinate, as shown in Figure 8c. Point 2, corresponding to 40 g/L feed concentration, is located above the complete separation zone, in the region where only the extract is pure. This is in good agreement with the experimental concentration profiles plotted in Figure 8b corresponding to an insufficient raffinate purity of 94%. Point 3 (80 g/L feed concentration) is located inside the complete separation zone, as is confirmed by the experimental profiles illustrated in Figure 8a. In the latter case, however, the zone of complete separation is very small and slight perturbations in the operating conditions can affect product purities.

Influence of the feed concentration

The separation productivity is defined as

$$PR = \frac{c_F Q_F}{PW}, \tag{15}$$

where c_F is the feed concentration, Q_F is the feed flow rate, and PW is the weight of the adsorbent phase contained in the SMB, for example, 1.5 kg of chiral phase. From this expression, it is clear that productivity increases with feed concentration. However, as the complete separation zone shrinks when the feed concentration increases, it becomes more and more difficult to select robust operating conditions. It was shown in Mazzotti et al. (1997) that, for a given feed concentration, PR is maximum at the vertex W (indicated for $c_F = 4$ g/L in Figure 9) of the triangular zone. This maximum productivity is plotted vs. feed concentration in Figure 10a for racemic mixture 2. No major increase of productivity is observed for feed concentrations larger than $c_{FA} = c_{FB} = c_F/2 = 10$ g/L. Actually, the asymptotic form of the productivity curve is very similar to the asymptotic evolution of the Langmuir isotherms, which is illustrated in Figure 10b. Hence, it is recommended that a feed concentration be selected, which corresponds to the smallest concentration leading to the saturation of the selective sites of the chiral phase. Of course, feed concentration will be limited by solubility.

Switching period

Once the feed concentration has been chosen, relative flow rates leading to a complete separation of the products and maximum productivity can be determined (minimum condition on m^1, maximum condition on m^4, and (m^2, m^3) given by the vertex W of the triangular zone). To obtain the SMB flow rates Q^j from the relative flow rates m^j, it is necessary to select a value for the switching period Δt. Again, this value will be chosen so as to achieve maximum productivity. In fact, productivity increases with the feed flow rate Q_F (Eq. 15) so that, when m^2 and m^3 are fixed (and so, Q_F/Q_S), higher productivity can only be achieved by increasing Q_S, that is, decreasing Δt. Hence, the switching period Δt should be as small as possible, considering the fact that, as Δt gets smaller, the several flow rates Q^j increase as the pressure drops in the system.

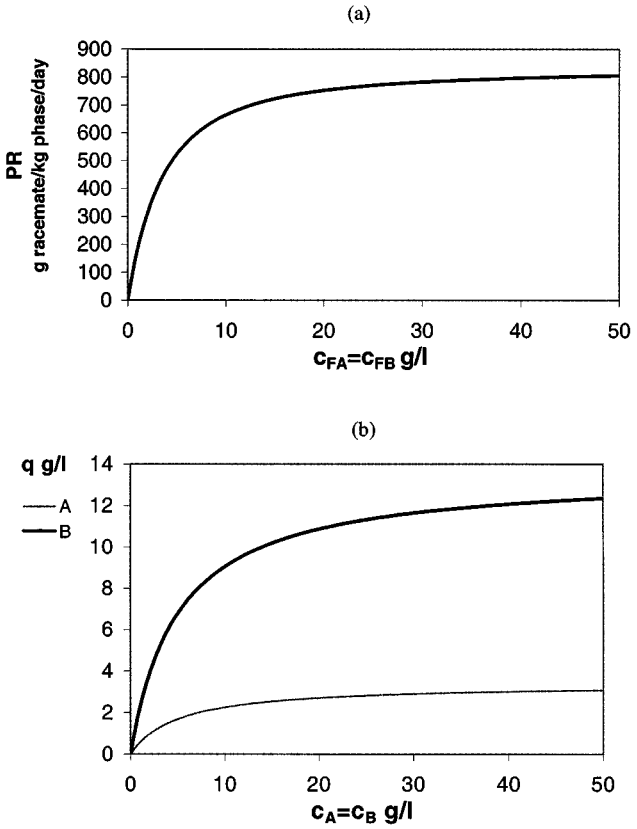

Figure 10. SMB separation of racemic mixture 2.

(a) Optimal productivity as a function of the feed concentration; (b) evolution of the Langmuir terms of the modified Langmuir isotherms.

Number of columns per zone

As it is apparent from Eq. 15, productivity increases when PW decreases. It is thus of interest to reduce the number of columns used in each SMB zone. Moreover, with fewer columns, smaller pressure drops occur, so that it is possible to operate the SMB process with a higher switching frequency, which also results in an increase in PR.

Consider an SMB configuration involving six columns: one column in zones 1 and 4, and two columns in zones 2 and 3 where the separation occurs (configuration 1-2-2-1). Figure 11a shows the zone of complete separation for racemic mixture 1 with a feed concentration $c_F = 40$ g/L. Figure 11b illustrates the internal concentration profiles corresponding to the optimal operating point W. In this case, however, due to relatively important dispersive phenomena, this operating point leads to some pollution of the products (purity level of the extract is only 96%). This divergence between theory and practice finds its origin in the fact that the analytical determination of the complete separation zone is based on the assumption that there is neither dispersion nor mass-transfer resistance. One way to remedy this situation is to increase the number of columns, as shown in Figure 11c, where the separation is performed with a 10-column SMB (configuration 1-6-2-1). In this latter case, the purity of the extract is now 99%, but the switching period had to be increased from 60 s to 85 s, with a consequent important loss of productivity

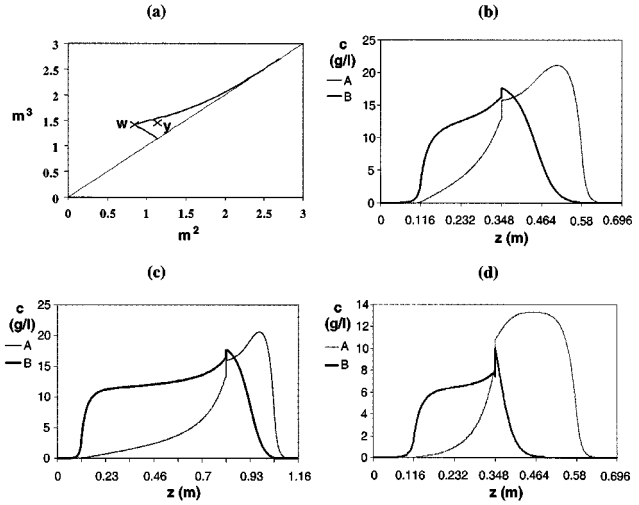

Figure 11. Compromise among purity, productivity, and solvent consumption illustrated with the SMB separation of racemic mixture 1 at $c_F = 40$ g/L.

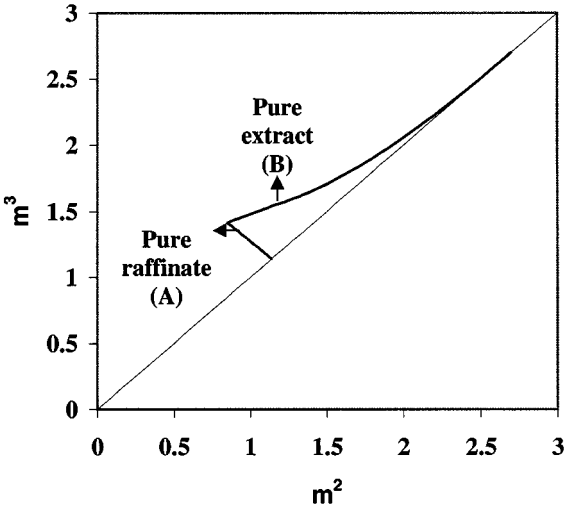

Figure 12. SMB operation outside the zone of complete separation.

Separation of racemic mixture 1 at $c_F = 40$ g/L. 1-2-2-1 SMB configuration, $\Delta t = 60$ s, $Q^1 = 337.4$ mL/min.

(from 3.10-kg racemate/kg phase/day to 1.31-kg racemate/kg phase/day). Another way to obtain pure products is to keep the same column configuration but to select an operating point located further away from the boundaries of the complete separation zone, such as point *y* (Figure 11a), leading to the internal concentration profiles given in Figure 11d. Although the product purities are satisfactory (> 99%), the choice of this operating point involves a very important increase in solvent consumption (from 171-kg liquid phase/kg racemate to 298 kg liquid phase/kg racemate). The example depicted in Figure 11 illustrates the inevitable compromise between purity, productivity, and solvent consumption. In the case of separations involving very expensive chiral adsorbent, economic criteria will be in favor of maximum productivity.

Outside the Zone of Complete Separation

For clinical tests, it is required to obtain both enantiomers with a high level of purity. For production purposes, however, only one of the enantiomers is usually of interest. In this section, operating points located outside the zone of complete separation—in a region of the (m^2, m^3) space where only the enantiomer of interest is pure—are investigated. Figure 12 shows the zone of complete separation for racemic mixture 1 at a feed concentration of 40 g/L and two arrows indicating the excursions in the pure extract or raffinate regions.

A first experimental observation is that, when the operating point (m^2, m^3) is outside but close to the zone of complete separation, the transient phase preceding the pollution of A or B can be relatively long. Table 2 illustrates this fact for several operating conditions.

In a first set of experiments, three operating points (*a*, *b*, and *c*) in the pure extract region are considered. These points correspond to $m^2 = 1.2$ and increasing values of $m^3 = 1.55$, 1.65, and 1.75, respectively. Point a, which is in the zone of complete separation, leads to a productivity of about 0.9-kg racemate/kg phase/day for both enantiomers. In points b and c, the extract productivity does not increase, but it is possible to transitorily obtain pure raffinate with an increased productivity (during a larger number of cycles for point b than for point c; see Table 2).

In a second set of experiments, three operating points (*d*, *e*, and *f*) in the pure raffinate region are considered, which correspond to $m^3 = 1.35$ and decreasing values of $m^2 = 0.9$, 0.8, and 0.7, respectively (see Table 2). Now, the raffinate productivity significantly increases from 1.2- to 1.67-kg racemate/kg phase/day when moving the SMB operating point from conditions d to f. Before pollution occurs, with increased productivity it is possible to transitorily obtain pure extract.

Therefore, very promising results, which correspond to increases in productivity of up to 40%, are obtained when operating the SMB process in the pure raffinate region. This

Table 2. SMB Separation of Racemic Mixture 1 at $c_F = 0.40$ g/L Configuration 1-2-2-1, $\Delta t = 60$ s, $Q^1 = 337.4$ mL/min

Point	*a*	*b*	*c*	*d*	*e*	*f*
m^2	1.2	1.2	1.2	0.9	0.8	0.7
m^3	1.55	1.65	1.75	1.35	1.35	1.35
$N_{cycle}(P > 99.9\%)$	∞	11	4	27	6	3
Productivity at the End of the Second Cycle						
PR_A (kg/kg/d)	0.86	1.22	1.57	0	0	0.05
PR_B (kg/kg/d)	0.71	0.72	0.72	1.21	1.47	1.73
Productivity at the End of the Last Cycle Before Pollution						
PR_A (kg/kg/d)	0.92	1.23	1.58	1.20	1.45	1.64
PR_B (kg/kg/d)	0.97	1.03	0.96	1.25	1.55	1.80
Steady-State Values of Purity and Productivity						
P_A (%)	100	81.3	72.6	100	100	100
P_B (%)	100	100	100	99.8	97.7	92.8
PR_A (kg/kg/d)	0.92	1.17	1.44	1.20	1.46	1.67
PR_B (kg/kg/d)	0.97	1.02	1.01	1.25	1.56	1.87

latter observation contradicts a recent study by Francotte et al. (1998), who conclude that operating the SMB process in the pure extract or raffinate regions has no positive effect on the productivity.

We attribute this observation to front and tail effects. In the pure extract (B component) region, the concentration front of B moves quickly, and most of B component added when passing from the complete separation zone to the pure B zone is going to the raffinate outlet. In the pure raffinate (A component) region, however, the diffuse back part of the concentration profile of A leads to much slower pollution of the extract.

Conclusions

In this work, the design features of an SMB process dedicated to the separation of racemates prior to clinical tests are presented. An equivalent countercurrent model is derived, in which mass-transfer kinetics are described by linear driving force models and the adsorption equilibrium relations are represented by modified Langmuir competitive isotherms. Based on a set of experiments performed with several of the SMB columns connected in series and operated in batch mode, unknown model parameters—total void fraction, dispersion coefficients, mass-transfer coefficients, and isotherm parameters—are estimated. In particular, a retention-time method allows a rapid estimation of the isotherm parameters, which serve as a starting point in a peak-fitting algorithm based on the minimization of a least-square criterion. This output-error criterion is defined implicitly through the numerical solution of an equilibrium-dispersion model of batch chromatography. Finally, the countercurrent model is validated by comparing detailed experimental concentration profiles, corresponding to various operating conditions, with the corresponding simulated profiles.

Following this modeling study, several issues related to the selection of optimal operating conditions are analyzed, both experimentally and in simulation:

- The influence of the feed concentration on the zone of complete separation, and the difficulty in selecting robust operating conditions at high feed concentrations, is highlighted. As a result of these investigations, it is suggested that the smallest concentration leading to the saturation of the selective sites of the chiral phase be chosen as maximum feed concentration.
- To achieve a high productivity (in kg racemate/kg phase/day) the number of columns and the switching period must be at a minimum. The switching period is limited by the pressure drop in the system, and thus by the number of columns.
- When dispersive phenomena are important, the zone of complete separation is reduced. Several alternative solutions exist, which necessarily compromise between purity, productivity, and solvent consumption. These alternatives can be advantageously evaluated using the simulation model.
- Depending on the component of interest, it might be appealing, in terms of productivity, to consider operating conditions outside the region of complete separation, leading only to the pure product of interest.

Notation

c_E = extract concentration
c_R = raffinate concentration
Q_E = extract flow rate
Q_R = raffinate flow rate
z = position along the SMB

Literature Cited

Cavoy, E., M.-F. Deltent, S. Lehoucq, and D. Miggiano, "Laboratory-Developed Simulated Moving Bed for Chiral Drug Separations. Design of the System and Separation of Tramadol Enantiomers," *J. Chromatog. A*, **769**, 49 (1997).

Francotte, E., P. Richert, M. Mazzotti, and M. Morbidelli, "Simulated Moving Bed Chromatographic Resolution of a Chiral Antitussive," *J. Chromatog. A*, **796**, 239 (1998).

Guiochon, G., S. Golshan-Shirazi, and A. M. Katti, *Fundamentals of Preparative and Nonlinear Chromatography*, Academic Press, San Diego (1994).

Hindmarsh, A. C., "ODEPACK, a Systematized Collection of ODE Solvers," *Scientific Computing*, R. S. Stepleman et al., eds., North-Holland, Amsterdam, p. 55 (1983).

Mazzotti, M., G. Storti, and M. Morbidelli, "Optimal Operation of Simulated Moving Bed Units for Nonlinear Chromatographic Separations," *J. Chromatog. A*, **769**, 3 (1997).

Negawa, M., and F. Shoji, "Optical Resolution by Simulated Moving Bed Adsorption Technology," *J. Chromatog.*, **590**, 113 (1992).

Nicoud, R. M., and A. Seidel-Morgenstern, "Adsorption Isotherms: Experimental Determination and Application to Preparative Chromatography," *Isol. Purif.*, **2**, 165 (1996).

Pais, L. S., J. M. Loureiro, and A. E. Rodrigues, "Modeling Strategies for Enantiomer Separation by SMB Chromatography," *AIChE J.*, **44**, (1998).

Ruthven, D. M., *Principles of Adsorption and Adsorption Processes*, Wiley, New York (1984).

Ruthven, D. M., and C. B. Ching, "Counter-Current and Simulated Counter-Current Adsorption Separation Processes," *Chem. Eng. Sci.*, **44**, 1011 (1989).

Schiesser, W. E., *The Numerical Method of Lines: Integration of Partial Differential Equations*, Academic Press, San Diego (1991).

Zhou, J. L., and A. Tits, *User's Guide for FFSQP Version 3.7: A FORTRAN Code for Solving Constrained Nonlinear (Minimax) Optimization Problems. Generating Feasible Iterates Satisfying All Inequality and Linear Constraints*, Univ. of Maryland, College Park (1997).

Manuscript received May 3, 1999, and revision received Sept. 27, 1999.